

# MITC9 Shell Finite Elements with Various Through-the-thickness Approximating Functions For the Analysis of Laminated Structures

Maria Cinefra\*, Guohong Li\* and Erasmo Carrera\*

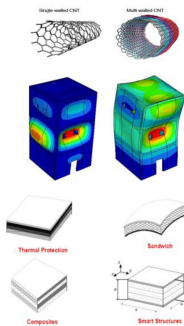
\*Department of Mechanical and Aerospace Engineering,  
Politecnico di Torino



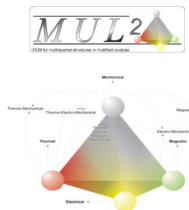
19<sup>th</sup> International Conference on Composite Structures, ICCS19  
6 September 2016, Porto

# MUL2 - Our Research Group

## MUL<sub>tilayered structures</sub>

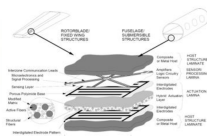
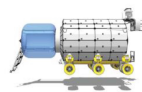
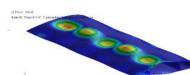


## [www.mul2.com](http://www.mul2.com)



[www.mul2.com](http://www.mul2.com)

## MUL<sub>field interaction</sub>



## Marie Curie Project on Composites



[www.fullcomp.net](http://www.fullcomp.net)

# FULLCOMP

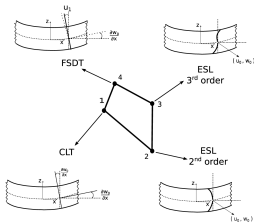
- FULLy integrated analysis, design, manufacturing and health-monitoring of COMPosite structures
- Funded by the European Commission under a *Marie Skłodowska-Curie* Innovative Training Networks grant for European Training Networks (ETN).
- The full spectrum of the design of composite structures will be dealt with, such as manufacturing, health-monitoring, failure, modeling, multiscale approaches, testing, prognosis, and prognostic.
- Research activities are aimed at engineering fields such as aeronautics, automotive, mechanical, wind energy and space.
- [www.fullcomp.net](http://www.fullcomp.net)

# FULLCOMP ESR1 – Variable, mixed, linear and nonlinear kinematic shell formulations including thermal, hygrothermal, piezo and magnetic effects

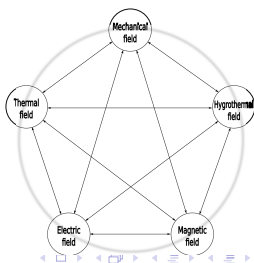
- Object: (Laminated) Shell (formulations)
- Methodology: CUF

**2D FEM Formulation** →  $\delta L_i = \delta u_{sj} k^{rsij} u_{ri}$

$$k_{xx}^{rsij} = (\lambda + 2G) \int_{\Omega} N_{i,x} N_{j,x} d\Omega \int_h F_{\tau} F_s dz \\ + G \int_{\Omega} N_{i,y} N_{j,d} d\Omega \int_h F_{\tau,z} F_{s,z} dz + G \int_V N_{i,y} N_{j,y} d\Omega \int_h F_{\tau} F_s dz; \\ k_{xy}^{rsij} = \lambda \int_{\Omega} N_{i,x} N_{j,y} d\Omega \int_h F_{\tau} F_s dz + G \int_{\Omega} N_{i,x} N_{j,y} d\Omega \int_h F_{\tau} F_s dz;$$



- Keyword: Variable kinematics**
  - Variable number of expansions: ESL-TYLN
  - Variable thickness function in different layers
- Keyword: Mixed kinematics**
  - Reissner's Mixed Variational Theorem
  - Mixed ESL-LW kinematic description on different FEM nodes
- Keyword: Linear and nonlinear**
  - Geometry non-linearity
  - Material non-linearity
- Keyword: Multifield effects**
  - Thermal, Hygroscopic, Electric, Magnetic, ...
  - Thermo-electrical, Electro-magnetic, Thermo-magnetic, ...

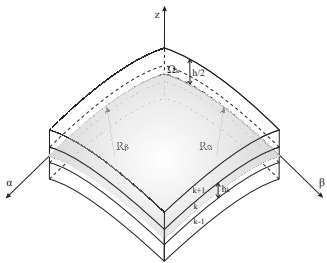


# Overview

- 1 Carrera Unified Formulation (CUF) and advanced 2D models.
- 2 Various thickness functions.
- 3 MITC9 element.
- 4 Numerical examples.
- 5 Conclusions.

## Doubly-curved Shell Geometry\*

Geometrical relations:



$$\epsilon_\alpha = \frac{1}{(1+z/R_\alpha)} \left( \frac{1}{A} \frac{\partial u}{\partial \alpha} + \frac{v}{AB} \frac{\partial A}{\partial \beta} + \frac{w}{R_\alpha} \right)$$

$$\epsilon_\beta = \frac{1}{(u+z/R_\beta)} \left( \frac{u}{AB} \frac{\partial B}{\partial \alpha} + \frac{1}{B} \frac{\partial v}{\partial \beta} + \frac{w}{R_\beta} \right)$$

$$\epsilon_z = \frac{\partial w}{\partial z}$$

$$\gamma_{\alpha\beta} = \frac{A(1+z/R_\alpha)}{B(1+z/R_\beta)} \frac{\partial}{\partial \beta} \left[ \frac{u}{A(1+z/R_\alpha)} \right] + \frac{B(1+z/R_\beta)}{A(1+z/R_\alpha)} \frac{\partial}{\partial \alpha} \left[ \frac{v}{B(1+z/R_\beta)} \right]$$

$$\gamma_{\alpha z} = \frac{1}{A(1+z/R_\alpha)} \frac{\partial w}{\partial \alpha} + A(1+z/R_\alpha) \frac{\partial}{\partial z} \left[ \frac{u}{A(1+z/R_\alpha)} \right]$$

$$\gamma_{\beta z} = \frac{1}{B(1+z/R_\beta)} \frac{\partial w}{\partial \beta} + B(1+z/R_\beta) \frac{\partial}{\partial z} \left[ \frac{v}{B(1+z/R_\beta)} \right]$$

$$H_\alpha = A(1+z/R_\alpha) \quad H_\beta = B(1+z/R_\beta)$$

Note:

- Constant radii of curvature  $R_\alpha$  and  $R_\beta$  lead to Lamé parameters  $A = B = 1$ .
- Exact shell geometry (middle-surface) curvature is described.

---

\* Leissa, A.W., 1973. NASA SP-288, Vibration of Shells.

## An Example: A Higher-order Deformation Theory for Plate Written in CUF

### - Displacement description

$$\begin{cases} u = u_0(x, y) & +z \cdot u_1(x, y) & + \dots & +z^N u_N(x, y) \\ v = v_0(x, y) & +z \cdot v_1(x, y) & + \dots & +z^N v_N(x, y) \\ w = w_0(x, y) & +z \cdot w_1(x, y) & + \dots & +z^N w_N(x, y) \end{cases}$$

$$\boldsymbol{u}^T = [u \quad v \quad w]^T = [\mathbf{F}_s u_s \quad \mathbf{F}_s v_s \quad \mathbf{F}_s w_s]^T = \mathbf{F}_s \boldsymbol{u}_s^T$$

$$\mathbf{F}_s(z) = z^{s-1} \quad s = 1, 2, \dots, N+1$$

### - FEM discretization

$$\boldsymbol{u}(x, y, z) = N_i(x, y) \cdot \boldsymbol{u}_i(z) = N_i(x, y) \cdot F_s(z) \cdot \boldsymbol{U}_{is}$$

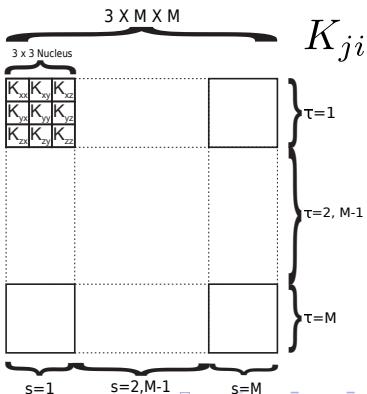
### - PVD

$$\boldsymbol{u}(x, y, z) = \mathbf{F}_\tau(z) \boldsymbol{u}_\tau(x, y) \quad \delta \boldsymbol{u}(x, y, z) = \mathbf{F}_s(z) \delta \boldsymbol{u}_s(x, y)$$

$$\begin{aligned} \delta L_{int} &= \int_V \delta \boldsymbol{\epsilon}^T \boldsymbol{\sigma} dV = \int_V \delta \boldsymbol{u}^T \mathbf{b}^T \mathbf{C} \boldsymbol{b} \boldsymbol{u} dV \\ &= \int_V \delta \boldsymbol{U}^T \mathbf{N}^T \mathbf{b}^T \mathbf{C} \mathbf{b} \mathbf{N} \boldsymbol{U} dV = \int_V \delta \boldsymbol{U}^T \mathbf{N}^T \mathbf{F}^T \mathbf{b}^T \mathbf{C} \mathbf{b} \mathbf{F} \mathbf{N} \boldsymbol{U} dV \\ &= \delta \boldsymbol{U}^T \cdot \int_V \delta \mathbf{N}^T \mathbf{F}^T \mathbf{b}^T \mathbf{C} \mathbf{b} \mathbf{F} \mathbf{N} dV \cdot \boldsymbol{U} = \delta \boldsymbol{U}^T \cdot \mathbf{K} \cdot \boldsymbol{U} \\ \delta L_{ext} &= \delta \boldsymbol{u}^T \mathbf{P} = \delta \boldsymbol{U}^T \mathbf{N}^T \mathbf{F}^T \mathbf{P} \end{aligned}$$

$$\mathbf{K}_{st}^{ij} = \int_V N_j \mathbf{F}_s \mathbf{b}^T \mathbf{C} \mathbf{b} \mathbf{F}_\tau N_i dV$$

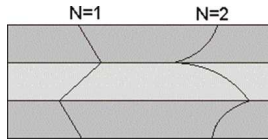
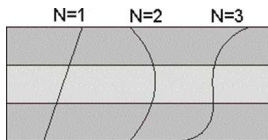
### Fundamental Nucleus



## CUF for Two Major Frameworks of Refined 2D Models

Equivalent-Single-Layer models (ESL)

Layer-Wise models (LW)



$$\boldsymbol{u} = F_0 \boldsymbol{u}_0 + F_1 \boldsymbol{u}_1 + \cdots + F_N \boldsymbol{u}_N$$

$$\boldsymbol{u}^k = F_t \boldsymbol{u}_t^k + F_b \boldsymbol{u}_b^k + F_r \boldsymbol{u}_r^k$$

Note:

–  $F_\tau$  defined on the whole through-thickness domain  $z$ .

Note:

–  $F_\tau$  defined on each layer thickness domain  $z^k$ ;  
– Continuity constraints at layer interfaces:  $\boldsymbol{u}_t^k = \boldsymbol{u}_b^{k+1}$ .

## CUF 2D Models Based on Series Expansion – Variable ESL Kinematics

- Taylor Series (ESL-TYL $\textcolor{red}{N}$ ) :  $F_\tau = z^n$ .

$$\begin{aligned} u &= u_1 + z u_2 + z^2 u_3 + \dots + z^N u_{N+1} \\ v &= u_1 + z v_2 + z^2 v_3 + \dots + z^N v_{N+1} \\ w &= \underbrace{w_1}_{n=0} + \underbrace{z w_2}_{n=1} + \underbrace{z^2 w_3}_{n=2} + \dots + \underbrace{z^N w_{N+1}}_{n=\textcolor{red}{N}} \\ \tau &= 1 \qquad \qquad \qquad \tau = 2 \qquad \qquad \qquad \tau = \textcolor{red}{N} + 1 \end{aligned}$$

- Exponential Series (ESL-EPN $\textcolor{red}{N}$ ) :  $F_\tau = e^{nz}$ .

$$\begin{aligned} u &= u_1 + e^z u_2 + e^{2z} u_3 + \dots + e^{Nz} u_{N+1} \\ v &= u_1 + e^z v_2 + e^{2z} v_3 + \dots + e^{Nz} v_{N+1} \\ w &= \underbrace{w_1}_{n=0} + \underbrace{e^z w_2}_{n=1} + \underbrace{e^{2z} w_3}_{n=2} + \dots + \underbrace{e^{Nz} w_{N+1}}_{n=\textcolor{red}{N}} \\ \tau &= 1 \qquad \qquad \qquad \tau = 2 \qquad \qquad \qquad \tau = \textcolor{red}{N} + 1 \end{aligned}$$

## CUF 2D Models Based on Series Expansion – Variable ESL Kinematics

- Hyperbolic Series (ESL-HPB**N**):  $\tau = 2k, F_\tau = \sinh(nz); \tau = 2k + 1, F_\tau = \cosh(nz)$ .

$$\begin{aligned} u &= \underbrace{u_1}_{n=0} + \underbrace{\sinh(z) u_2}_{n=1} + \underbrace{\cosh(z) u_3}_{n=2} + \underbrace{\sinh(2z) u_4}_{n=3} + \dots \\ v &= \underbrace{u_1}_{\tau=1} + \underbrace{\sinh(z) v_2}_{\tau=2} + \underbrace{\cosh(z) v_3}_{\tau=3} + \underbrace{\sinh(2z) v_4}_{\tau=4} + \dots \\ w &= \underbrace{w_1}_{\tau=1} + \underbrace{\sinh(z) w_2}_{\tau=2} + \underbrace{\cosh(z) w_3}_{\tau=3} + \underbrace{\sinh(2z) w_4}_{\tau=4} + \dots \end{aligned}$$

- Trigonometric Series (ESL-TRG**N**):  $\tau = 2k, F_\tau = \sin(nz); \tau = 2k + 1, F_\tau = \cos(nz)$ .

$$\begin{aligned} u &= \underbrace{u_1}_{n=0} + \underbrace{\sin(z) u_2}_{n=1} + \underbrace{\cos(z) u_3}_{n=2} + \underbrace{\sin(2z) u_4}_{n=3} + \dots \\ v &= \underbrace{u_1}_{\tau=1} + \underbrace{\sin(z) v_2}_{\tau=2} + \underbrace{\cos(z) v_3}_{\tau=3} + \underbrace{\sin(2z) v_4}_{\tau=4} + \dots \\ w &= \underbrace{w_1}_{\tau=1} + \underbrace{\sin(z) w_2}_{\tau=2} + \underbrace{\cos(z) w_3}_{\tau=3} + \underbrace{\sin(2z) w_4}_{\tau=4} + \dots \end{aligned}$$

- Zig-Zag model (ESL-XXX**NZ**):  $F_{N+2} = (-1)^k \zeta_k \mathbf{u}_Z$  (*Murakami's function*)

$$\mathbf{u} = F_1 \mathbf{u}_1 + \dots + F_{N+1} \mathbf{u}_{N+1} + (-1)^k \zeta_k \mathbf{u}_Z.$$

## CUF 2D Models Based on Interpolation Polynomials – Variable LW Kinematics

- Kinematics of Layer-Wise Models (LW $\textcolor{red}{N}$ ):

$$\begin{aligned} u &= F_1 u_1 + F_2 u_2 + \dots + F_{N+1} u_{N+1} \\ v &= F_1 u_1 + F_2 v_2 + \dots + F_{N+1} v_{N+1} \\ w &= \underbrace{F_1 w_1}_{\tau = 1} + \underbrace{F_2 w_2}_{\tau = 2} + \dots + \underbrace{F_{N+1} w_{N+1}}_{\tau = \textcolor{red}{N} + 1} \end{aligned}$$

- Lagrange (LW-LGR $\textcolor{red}{N}$ ):  $F_\tau(\zeta_k) = \prod_{i=0, i \neq s}^N \frac{\zeta_k - \zeta_{k_i}}{\zeta_{k_s} - \zeta_{k_i}}, -1 \leq \zeta_k \leq -1$

*Note: Each  $\zeta_{k_s}$  or  $\zeta_{k_i}$  indicates a "Sampling Surface" with physical displacements.*

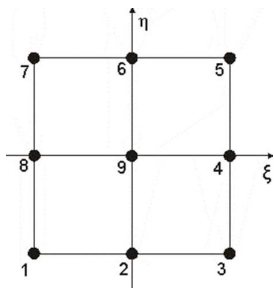
- Legendre (LW-LGD $\textcolor{red}{N}$ ):  $F_t = \frac{P_0 + P_1}{2}, F_b = \frac{P_0 - P_1}{2}, F_r = P_r - P_{r-2}$

*Note:  $P_0 = 1, P_1 = \zeta_k, NP_N = (2N - 1)\zeta_k P_{N-1} - (N - 1)P_{N-2}, -1 \leq \zeta_k \leq -1$*

- Chebyshev (First Kind) (LW-CBS $\textcolor{red}{N}$ ):  $F_t = \frac{T_0 + T_1}{2}, F_b = \frac{T_0 - T_1}{2}, F_r = T_r - T_{r-2}$

*Note:  $T_0 = 1, T_1 = \zeta_k, T_N = 2\zeta_k T_{N-1} - T_{N-2}, -1 \leq \zeta_k \leq -1$*

## 9-node Shell Finite Element



$$N_1 = \frac{1}{4}(\xi^2 - \xi)(\eta^2 - \eta), \quad N_2 = \frac{1}{4}(1 - \xi^2)(\eta^2 - \eta)$$

$$N_3 = \frac{1}{4}(\xi^2 + \xi)(\eta^2 - \eta), \quad N_4 = \frac{1}{4}(\xi^2 + \xi)(1 - \eta^2)$$

$$N_5 = \frac{1}{4}(\xi^2 + \xi)(\eta^2 + \eta), \quad N_6 = \frac{1}{4}(1 - \xi^2)(\eta^2 + \eta)$$

$$N_7 = \frac{1}{4}(\xi^2 - \xi)(\eta^2 + \eta), \quad N_8 = \frac{1}{4}(\xi^2 - \xi)(1 - \eta^2)$$

$$N_9 = (1 - \xi^2)(1 - \eta^2)$$

## Mixed Interpolation of Tensorial Components

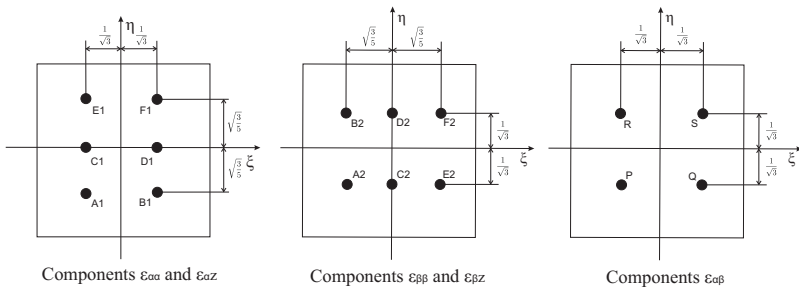


Figure: Tying points for the MITC9 shell element.

$$N_{m1} = [N_{A1}, N_{B1}, N_{C1}, N_{D1}, N_{E1}, N_{F1}]$$

$$N_{m2} = [N_{A2}, N_{B2}, N_{C2}, N_{D2}, N_{E2}, N_{F2}]$$

$$N_{m3} = [N_P, N_Q, N_R, N_S]$$

$$\boldsymbol{\epsilon}_p = \begin{bmatrix} \epsilon_{\alpha\alpha} \\ \epsilon_{\beta\beta} \\ \epsilon_{\alpha\beta} \end{bmatrix} = \begin{bmatrix} N_{m1} & 0 & 0 \\ 0 & N_{m2} & 0 \\ 0 & 0 & N_{m3} \end{bmatrix} \begin{bmatrix} \epsilon_{\alpha\alpha m1} \\ \epsilon_{\beta\beta m2} \\ \epsilon_{\alpha\beta m3} \end{bmatrix}$$

$$\boldsymbol{\epsilon}_n = \begin{bmatrix} \epsilon_{\alpha z} \\ \epsilon_{\beta z} \\ \epsilon_{zz} \end{bmatrix} = \begin{bmatrix} N_{m1} & 0 & 0 \\ 0 & N_{m2} & 0 \\ 0 & 0 & 1 \end{bmatrix} \begin{bmatrix} \epsilon_{\alpha z m1} \\ \epsilon_{\beta z m2} \\ \epsilon_{zz} \end{bmatrix}$$

## 3D Constitutive Equations

*Stress-strain relations for an orthotropic material:*

$$\sigma_p^k = \mathbf{C}_{pp}^k \epsilon_p^k + \mathbf{C}_{pn}^k \epsilon_n^k$$

$$\sigma_n^k = \mathbf{C}_{np}^k \epsilon_p^k + \mathbf{C}_{nn}^k \epsilon_n^k$$

where

$$\mathbf{C}_{pp}^k = \begin{bmatrix} C_{11}^k & C_{12}^k & C_{16}^k \\ C_{12}^k & C_{22}^k & C_{26}^k \\ C_{16}^k & C_{26}^k & C_{66}^k \end{bmatrix} \quad \mathbf{C}_{pn}^k = \begin{bmatrix} 0 & 0 & C_{13}^k \\ 0 & 0 & C_{23}^k \\ 0 & 0 & C_{36}^k \end{bmatrix}$$

$$\mathbf{C}_{np}^k = \begin{bmatrix} 0 & 0 & 0 \\ 0 & 0 & 0 \\ C_{13}^k & C_{23}^k & C_{36}^k \end{bmatrix} \quad \mathbf{C}_{nn}^k = \begin{bmatrix} C_{55}^k & C_{45}^k & 0 \\ C_{45}^k & C_{44}^k & 0 \\ 0 & 0 & C_{33}^k \end{bmatrix}$$

## Case 1<sup>†</sup>: Plate, [0°/90°/0°], $a/h = 2$ and 100, loaded on top surface

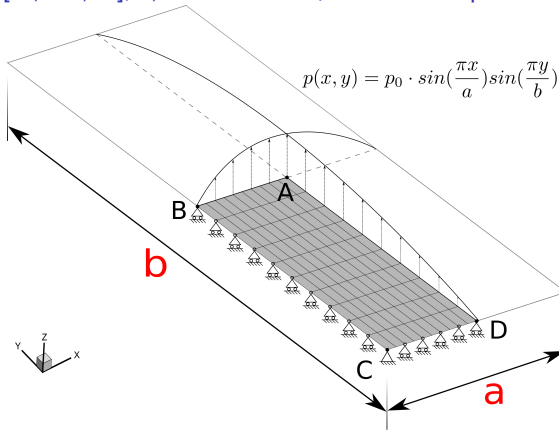
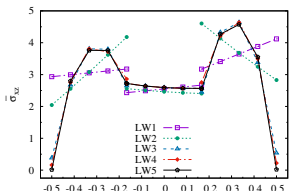


Figure: 2D FEM 1/4 model with symmetry for the composite plate.

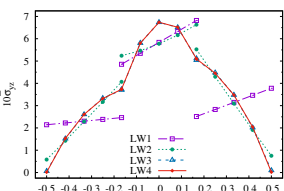
<sup>†</sup> Pagano, N.J., 1970. Exact solutions for rectangular bidirectional composites and sandwich plates: Journal of Composite Materials, Vol 4, pp 20-34 (January 1970). Composite, 1(4), p.257.

## Plate, [0°/90°/0°], $a/h = 2$ and 100, $\bar{\sigma}_{xz}$ and $\bar{\sigma}_{yz}$ variation through $\bar{z}$ , with $LWN^*$

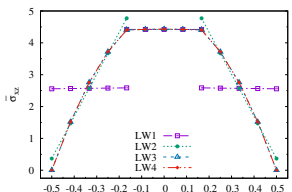
\*Note: LW-LGRN, -LGDN, -CBSN lead to the same results within the numerical tolerance, uniformly denoted as  $LWN$ .



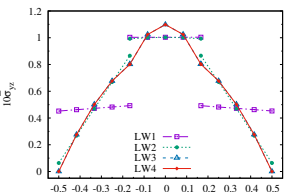
(a)  $\bar{\sigma}_{xz}$ ,  $a/h = 2$ , Point B



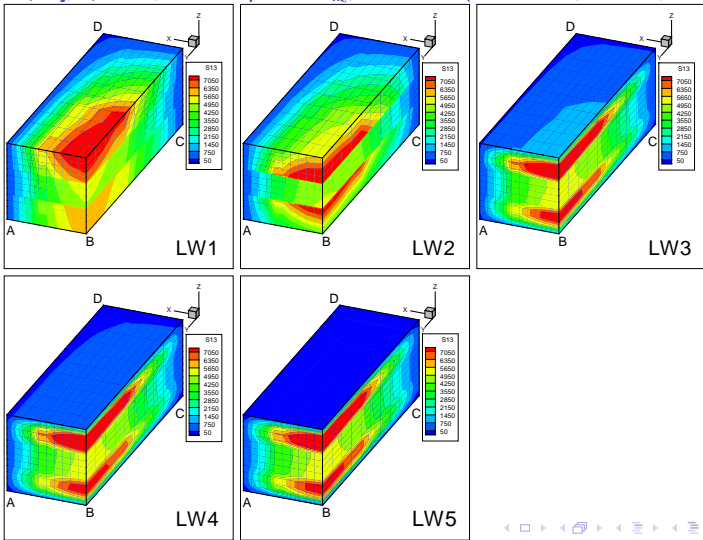
(b)  $\bar{\sigma}_{xz}$ ,  $a/h = 2$ , Point D



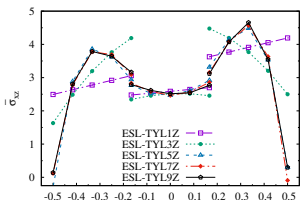
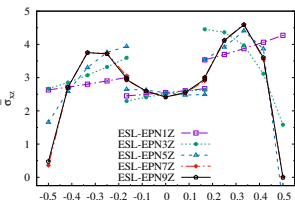
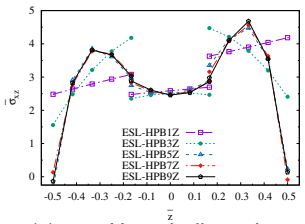
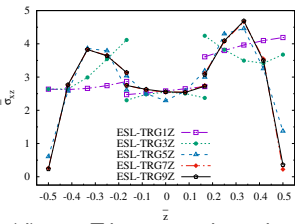
(c)  $\bar{\sigma}_{xz}$ ,  $a/h = 100$ , Point B

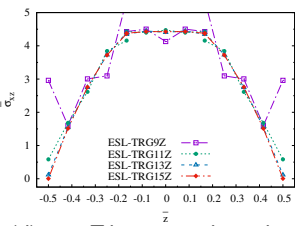
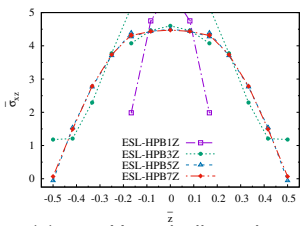
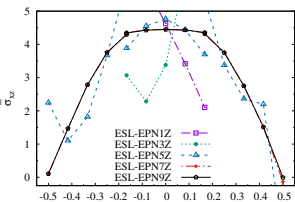
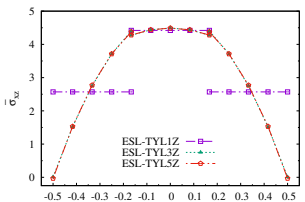


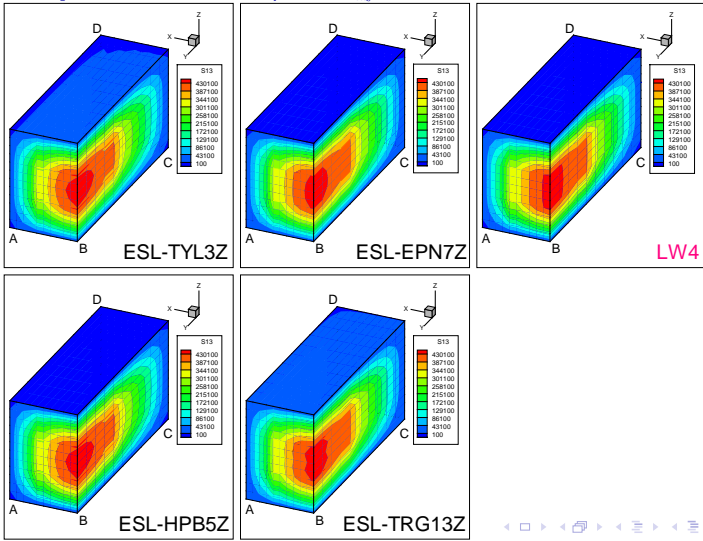
(d)  $\bar{\sigma}_{yz}$ ,  $a/h = 100$ , Point D

Plate,  $[0^\circ/90^\circ/0^\circ]$ ,  $a/h = 2$ , contour plot of  $\sigma_{xz}$ , with LWN (LW-LGRN, -LGDN, -CBSN)

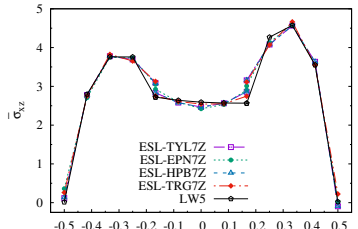
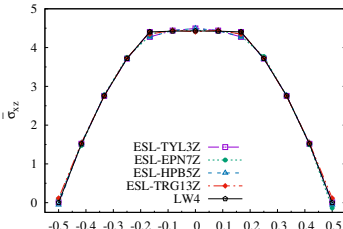
Plate, [0°/90°/0°],  $a/h = 2$ , variation of  $\bar{\sigma}_{xz}$  through  $\bar{z}$  at Point B, with , with ESLNZ

(a)  $\bar{\sigma}_{xz}$ , Taylor series.(b)  $\bar{\sigma}_{xz}$ , Exponential series.(c)  $\bar{\sigma}_{xz}$ , Hyperbolic series.(d)  $\bar{\sigma}_{xz}$ , Trigonometric series.

Plate, [0°/90°/0°],  $a/h = 100$ , variation of  $\bar{\sigma}_{xz}$  through  $\bar{z}$  at Point B, with ESLNZ

Plate,  $[0^\circ/90^\circ/0^\circ]$ ,  $a/h = 100$ , contour plot of  $\sigma_{xz}$ , with ESLNZ and LW4

## A Summary of Case 1

(a)  $a/h = 2$ (b)  $a/h = 100$ 

$a/h$	Kinematics	$\bar{u}_z$ $A, z = 0$	$\bar{\sigma}_{xx}$ $A, z = \frac{h}{2}$	$\bar{\sigma}_{yy}$ $A, z = \frac{h}{6}$	$10\bar{\sigma}_{xy}$ $C, z = -\frac{h}{2}$	$\bar{\sigma}_{xz}$ $B, z = 0$	$10\bar{\sigma}_{yz}$ $D, z = 0$	$\bar{\sigma}_{zz}$ $A, z = \frac{h}{2}$
2	ESL-TYL7Z	8.161	2.150	1.881	5.558	2.466	6.662	1.015
	ESL-EPN7Z	8.158	2.147	1.911	5.546	2.422	6.518	1.003
	ESL-HPB7Z	8.161	2.150	1.882	5.559	2.465	6.651	1.014
	ESL-TRG7Z	8.163	2.150	1.900	5.559	2.542	6.796	1.020
	LW5	8.166	2.150	2.310	5.571	2.592	6.732	1.002
	Pagano(1970)	8.17	2.13	2.30	5.48	2.57	6.68	1.0000
100	ESL-TYL3Z	0.5077	0.6294	0.2537	0.8458	4.494	1.083	1.810
	ESL-EPN7Z	0.5077	0.6294	0.2544	0.8458	4.447	0.9407	-1.073
	ESL-HPB5Z	0.5077	0.6294	0.2539	0.8458	4.496	1.121	-0.1260
	ESL-TRG13Z	0.5077	0.6294	0.2543	0.8458	4.406	1.042	1.253
	LW4	0.5077	0.6294	0.2551	0.8458	4.429	1.098	1.018
	Pagano(1970)	0.508	0.624	0.253	0.83	4.39	1.08	1.000

## Case 2<sup>‡</sup>: Cylindrical shell, [0°/90°], $R_\beta/h = 2$ and 100, loaded on bottom surface

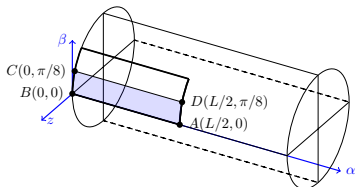


Figure: Geometry feature of the cylindrical shell.

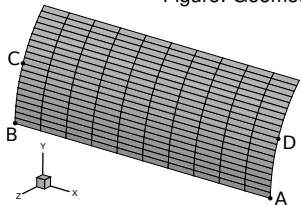


Figure: 2D FEM 1/16 model

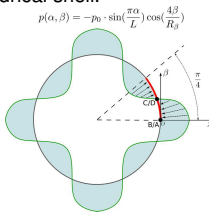
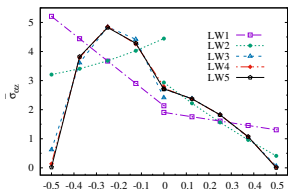


Figure: Loading profile on cross section

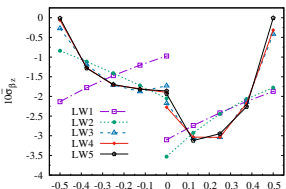
<sup>‡</sup>Varadan, T.K., 1991. Bending of laminated orthotropic cylindrical shells - an elasticity approach. Composites Structures, 17(2), pp.141-156.

## Shell, [0°/90°], $R_\beta/h = 2$ and 100, $\bar{\sigma}_{\alpha z}$ and $\bar{\sigma}_{\beta z}$ variation through $\bar{z}$ , with $LWN^*$

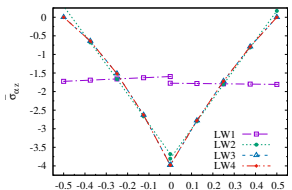
\*Note: LW-LGRN, -LGDN, -CBSN lead to the same results within the numerical tolerance, uniformly denoted as  $LWN$ .



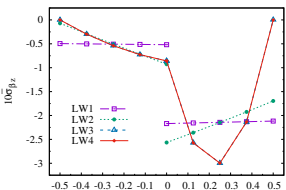
(a)  $\bar{\sigma}_{\alpha z}$ ,  $R_\beta/h = 2$ , Point B



(b)  $\bar{\sigma}_{\beta z}$ ,  $R_\beta/h = 2$ , Point D

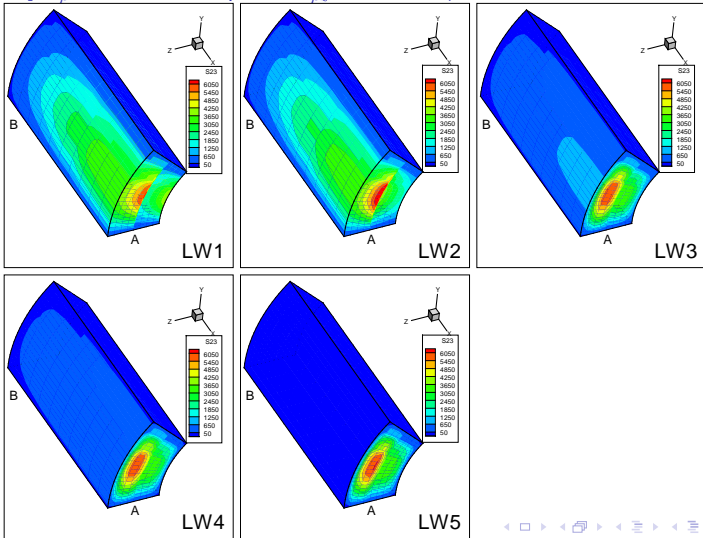


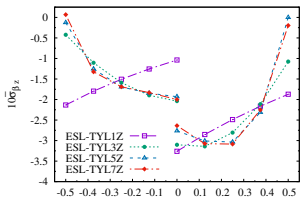
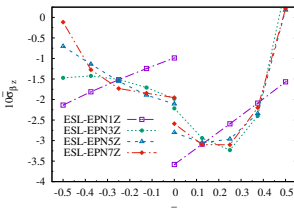
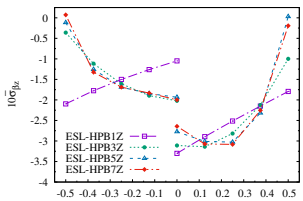
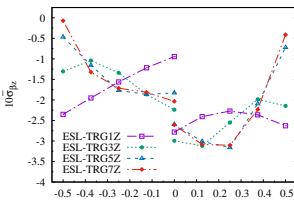
(c)  $\bar{\sigma}_{\alpha z}$ ,  $R_\beta/h = 100$ , Point B

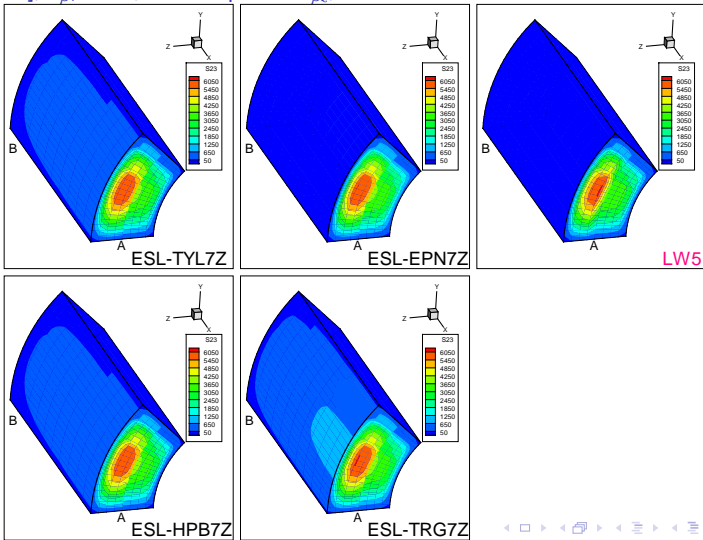


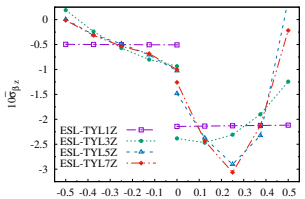
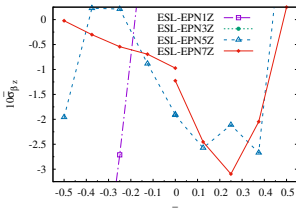
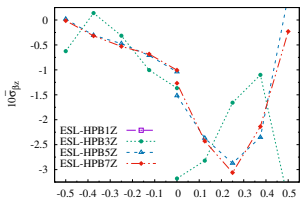
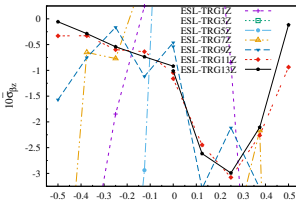
(d)  $\bar{\sigma}_{\beta z}$ ,  $R_\beta/h = 100$ , Point D

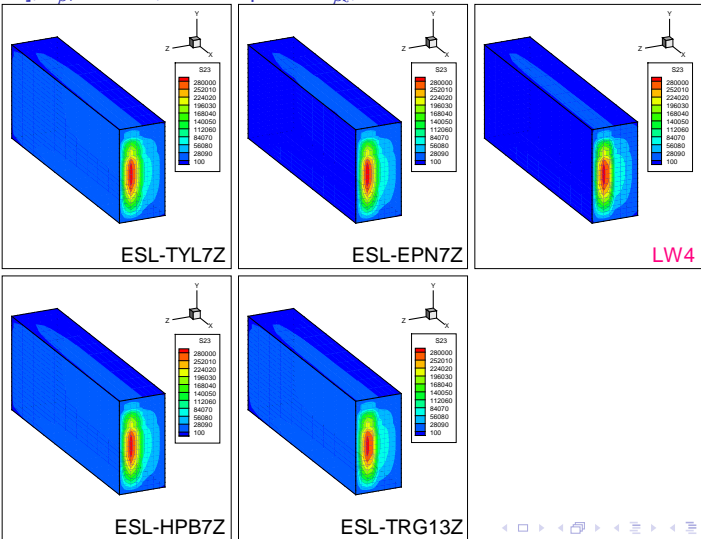
Shell, [0°/90°],  $R_\beta/h = 2$ , contour plot of  $\sigma_{\beta z}$ , with LWN (LW-LGRN, -LGDN, -CBSN)



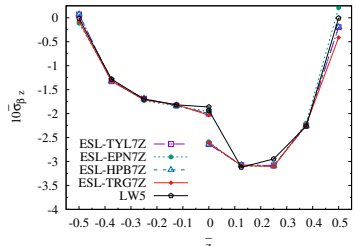
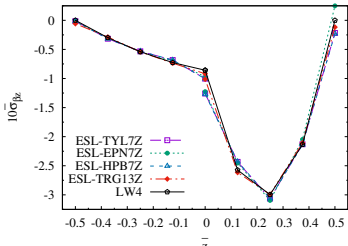
Shell, [0°/90°],  $R_\beta/h = 2$ ,  $\bar{\sigma}_{\beta z}$  variation through  $\bar{z}$  at Point D, with ESLNZ(a)  $\bar{\sigma}_{\beta z}$ , Taylor series.(b)  $\bar{\sigma}_{\beta z}$ , Exponential series.(c)  $\bar{\sigma}_{\beta z}$ , Hyperbolic series.(d)  $\bar{\sigma}_{\beta z}$ , Trigonometric series.

Shell, [0°/90°],  $R_\beta/h = 2$ , contour plot of  $\sigma_{\beta z}$ , with ESLNZ and LW5

Shell, [0°/90°],  $R_\beta/h = 100$ ,  $\bar{\sigma}_{\beta z}$  variation through  $\bar{z}$  at Point D, with ESLNZ(a)  $\bar{\sigma}_{\beta z}$ , Taylor series.(b)  $\bar{\sigma}_{\beta z}$ , Exponential series.(c)  $\bar{\sigma}_{\beta z}$ , Hyperbolic series.(d)  $\bar{\sigma}_{\beta z}$ , Trigonometric series.

Shell, [0°/90°],  $R_\beta/h = 100$ , contour plot of  $\sigma_{\beta z}$ , with ESLNZ and LW4

## A Summary of Case 2

(a)  $a/h = 2$ (b)  $a/h = 100$ 

$R_\beta/h$	Kinematics	$\bar{u}_z$	$\bar{\sigma}_{\alpha\alpha}$	$\bar{\sigma}_{\beta\beta}$	$10\bar{\sigma}_{\alpha\beta}$	$\bar{\sigma}_{\alpha z}$	$10\bar{\sigma}_{\beta z}$	$\bar{\sigma}_{zz}$
		$A, z = 0$	$A, z = \frac{h}{2}$	$A, z = \frac{h}{2}$	$C, z = \frac{h}{2}$	$B, z = -\frac{h}{4}$	$D, z = \frac{h}{4}$	$A, z = \frac{h}{4}$
2	ESL-TYL7Z	1.3965	0.2432	0.9814	2.7216	4.8546	-3.0846	-0.2845
	ESL-EPN7Z	1.3974	0.2691	0.9870	2.7261	4.8586	-3.1023	-0.2883
	ESL-HPB7Z	1.3963	0.2431	0.9815	2.7215	4.8523	-3.0833	-0.2846
	ESL-TRG7Z	1.3981	0.2464	0.9778	2.7193	4.8990	-3.1034	-0.2819
	LW5	1.4035	0.2558	0.9858	2.7288	4.8244	-2.9469	-0.3124
	Varadhan(1991)	1.4034	0.2511	0.9775	2.685	4.786	-2.931	-0.31
100	ESL-TYL7Z	0.1367	0.1884	0.5605	-1.8485	-1.4087	-3.0645	-8.0118
	ESL-EPN7Z	0.1367	0.1886	0.5606	-1.8485	-1.4416	-3.0967	-7.9314
	ESL-HPB7Z	0.1367	0.1884	0.5605	-1.8485	-1.4158	-3.0616	-7.9900
	ESL-TRG13Z	0.1367	0.1887	0.5606	-1.8485	-1.5274	-2.9919	-7.5984
	LW4	0.1367	0.1887	0.5606	-1.8485	-1.5171	-2.9968	-7.7626
	Varadhan(1991)	0.1367	0.1871	0.5560	-1.819	-1.512	2.972	-7.71

# Main Conclusions and Perspectives

- 1 CUF provides a general way to integrate various approximation theories to obtain refined FEM element with variable kinematics for analysis of multi-layered structures.
- 2 MITC9 shell element adopted is free of shear and membrane locking.
- 3 With sufficient number of expansions, all the thickness-functions studied can achieve good approximation of displacements and stresses, and the number of essential expansions depends on the specific situation.
- 4 In the case of LW approach, interpolation polynomials of Lagrange, Legendre and Chebyshev provide the same numerical results if the polynomials adopted are of the same order.
- 5 For the cases studied, LW4 is sufficient to capture the transverse shear stress variation, while LW5 is recommended for thick laminated structures.
- 6 In different cases, ESL models with various thickness functions show different convergence rate with the increase of expansion number, especially for thin laminated structures.
- 7 Trigonometric series tend to use more expansions to achieve convergence in the cases studied.

## Future extensions

- Variable LW-ESL kinematics.
- Application in multi-field problems.

# MITC9 Shell Finite Elements with Various Through-the-thickness Approximating Functions For the Analysis of Laminated Structures

Maria Cinefra\*, Guohong Li\* and Erasmo Carrera\*

\*Department of Mechanical and Aerospace Engineering,  
Politecnico di Torino



19<sup>th</sup> International Conference on Composite Structures, ICCS19  
6 September 2016, Porto